

## Mullite Formation from Mixtures of Alumina and Silica Sols: Mechanism and pH Effect

Carla C. Osawa and Celso A. Bertran\*

Instituto de Química, Universidade Estadual de Campinas, CP 6154, 13083-970 Campinas - SP, Brazil

Este trabalho relata o efeito do pH no processo de formação de mulita a partir de misturas de sóis de alumina e sílica. O pH das misturas determina as cargas das superfícies das partículas e afeta suas interações e distribuições. A formação de mulita a partir de precursores amorfos na razão molar de 1:3, preparados pela mistura dos sóis, não foi afetada pelo pH. Neste caso, a concentração excessiva de sílica determinou sua distribuição ao redor da alumina, o que levou à formação de mulita tetragonal, conforme o mecanismo de Sundaresan e Aksay. Entretanto, para a formação de mulita a partir de precursores com Al:Si = 3:1, o pH desempenhou um papel muito importante nas interações entre partículas de alumina e de sílica, bem como nas espécies predominantes de alumínio. Em pH 1, íons  $\text{Al}^{3+}$  octaédricamente coordenados predominaram no sol de alumina enquanto que íons  $\text{Al}^{3+}$  tetraédricamente coordenados predominaram no sol a pH ~6. As interações entre as partículas de sílica e de alumina e suas distribuições nesses precursores determinaram a temperatura mínima de formação de mulita ortorrômbica.

This work reports the effect of pH on the process of mullite formation from mixtures of alumina and silica sols. The pH of the mixtures determines the charges of particle surfaces and affects their interactions and distributions. Mullite formation from amorphous precursors with an Al:Si molar ratio of 1:3, prepared from the sols mixture, was not affected by pH. In this case, the higher concentration of silica determined its distribution around alumina, which led to tetragonal mullite formation, according to the Sundaresan and Aksay mechanism. However, for mullite formation from precursors with Al:Si = 3:1, the pH played an important role on the interactions between alumina and silica particles, as well as on the predominant aluminum species. At pH 1, octahedrally coordinated  $\text{Al}^{3+}$  ions predominated in the alumina sol while tetrahedrally coordinated  $\text{Al}^{3+}$  ions predominated in the sol at pH ~6. The interactions between silica and alumina particles and their distributions in these precursors determined the minimum temperature required for orthorhombic mullite formation.

**Keywords:** pH effect, mullite formation, alumina sol, silica sol

### Introduction

Mullite ( $3\text{Al}_2\text{O}_3 \cdot 2\text{SiO}_2$ ) is a very important ceramic material, with high temperature applications, due to its excellent mechanical properties, such as high strength, low thermal expansion coefficient, low thermal conductivity, high thermal shock resistance and creep resistance.<sup>1-6</sup>

Mullite is also an interesting model for the development of new procedures of ceramic material synthesis, due to the simplicity of its composition.<sup>7</sup> This ceramic material is composed solely of silicon, aluminum and oxygen, and is the only crystalline phase of the  $\text{Al}_2\text{O}_3$ - $\text{SiO}_2$  system stable at atmospheric pressure.<sup>1, 8-10</sup>

Studies of mullite formation from alumina and silica sols can be useful to evaluate the interactions of alumina and silica particles in an aqueous medium, as a function of the pH, and, consequently, the effect of these interactions on mullite synthesis.

In this work, mullite formation was employed as a model to investigate particle interactions in mixtures composed of two different sols (alumina and silica sols) where the charges on the particle surfaces are determined by the pH value. Particles of like charge repel each other, whereas particles of opposite charge attract each other and are susceptible to promoting heterocoagulation. Heterocoagulation is a particular situation generally found in processing mixtures of sols at a pH between the isoelectric points of each component.<sup>11</sup> For instance, a system composed of alumina and silica sols, which have

\* e-mail: bertran@iqm.unicamp.br

isoelectric points, respectively, of  $\sim 2$ <sup>12</sup> and  $\sim 7$ <sup>11</sup>, is prone to heterocoagulation at pH 4. In this case, the pH determines the charges of alumina and silica particles and, as a consequence, affect the distribution of the alumina and silica on the mullite precursor prepared from a mixture of these two sols.

Mixtures consisting of two kinds of sols that provide ceramic material precursors are not widely studied and do not receive the attention they deserve. In a system composed of more than one kind of particle, the nature of the interactions that predominate differ significantly from the interactions of a system composed of particles of the same kind.<sup>13</sup> The interactions of particles of the same kind are well described by the DLVO theory,<sup>14</sup> whereas there is not a suitable model that explains the interactions among particles in a system composed of different kinds of particles.

As mullite is considered a model for the sol-gel synthesis of ceramic materials, it is relevant to study mullite synthesis from mixtures of sols under this approach. Besides, the interactions between particles in a mixture of sols are a challenge from the experimental and theoretical point of view. Papers correlating the distribution of particles in a precursor or the uniformity of a ceramic material as a function of the pH of the sol-gel synthesis are rare. On the other hand, the sol-gel route for mullite synthesis without pH control has been the subject of numerous papers.<sup>4,7,8,15-25</sup> The vast majority of these papers about mullite produced by the sol-gel method use TEOS (tetraethylorthosilicate) and aluminum alkoxides or salts.<sup>17,19,20,25</sup> There are only a few papers that use mixtures of alumina and silica sols in aqueous dispersion to prepare amorphous mullite precursors or crystalline mullite.<sup>24</sup>

The sol-gel method is reported as a synthetic route capable of providing a good mixing or uniformity of the starting materials, at the nanoscale, resulting in a very homogeneous distribution of the components. As a consequence of the high degree of homogeneity of a precursor, the temperature required for mullite formation is relatively low (from  $\sim 1000$  to  $1350$  °C),<sup>2,7,15,18-24</sup> if compared to traditional methods, such as mixtures of reactive powders.

The gels obtained from mullite sol-gel synthesis can be classified as single-phase and diphasic gels, based on their chemical homogeneities (short distance atomic arrangement) and their resulting behaviors.<sup>23</sup>

Single-phase gels exhibit molecular mixing of aluminum and silicon and present Al-O-Si bonds.<sup>21</sup> In this case, the mullite precursors obtained from them remain amorphous until the mullite phase is crystallized, at approximately  $1000$  °C.<sup>17</sup>

On the other hand, diphasic gels present domains rich in alumina and in silica and are generally obtained from mixtures of alumina and silica sols or silica sol and aluminum salts.<sup>20</sup> In some mullite precursors obtained from diphasic gels, mullite can be formed from a solid state reaction between either amorphous silica and transition aluminas ( $\delta$ -,  $\gamma$ - or  $\theta$ -alumina)<sup>18,19</sup> or amorphous silica and the spinel phase.<sup>21</sup> It is also possible that these two reactional routes coexist.<sup>7</sup> Mullite crystallization from precursors obtained from diphasic gels occurs typically between  $\sim 1150$  and  $1350$  °C.<sup>23,24</sup> In this case, mullite formation can be adequately represented by a mechanism proposed by Sundaresan and Aksay,<sup>18</sup> which consists of nucleation and growth processes.

According to Sundaresan and Aksay,<sup>18</sup> there are two pure phases in the mullite precursors. One phase contains transition alumina while the other phase consists of amorphous silica. Alumina particles dissolve in the amorphous silica phase, under thermal treatment, leading to the formation of an aluminosilicate matrix. When the alumina concentration present in the matrix exceeds a critical nucleation concentration, mullite nuclei are formed. These nuclei grow with alumina particle incorporation and the growth rate of mullite nuclei is governed by alumina dissolution in the amorphous phase.

Although this mechanism is well established and explains mullite formation, it seems that this model has received little attention, since there are few experimental results that have been published to support it.

One aim of this work was to report experimental results that can be analyzed by the mechanism proposed by Sundaresan and Aksay for mullite formation using samples prepared by the sol-gel method in aqueous medium. Mixtures of alumina and silica sols at different pH values under the condition of excessive silica (Al:Si molar ratio of 1:3) and at the stoichiometric mullite composition (Al:Si = 3:1) were studied.

The effect of pH on mullite formation was analyzed by the minimum temperature required to transform amorphous mullite precursors into crystalline mullite and is related to the interactions among alumina and silica particles in the mixtures of alumina and silica sols.

## Experimental

### Preparation of sols

Alumina sol<sup>24,26</sup> was prepared from a saturated aqueous solution of aluminum nitrate nonahydrate ( $\text{Al}(\text{NO}_3)_3 \cdot 9\text{H}_2\text{O}$ ) (PA, Vetec) and urea (PA, Reagen), with an  $\text{Al}^{3+}$ :urea molar ratio of 1:13 at pH 2. This solution was kept in a  $22$  °C

water bath for 1 h, filtered through a 0.45 mm Millipore filter to remove all the solid contaminants, and then kept at  $\sim 80$  °C in an erlenmeyer covered with aluminum foil until the solution reached a pH value near 6. In order to obtain an alumina sol at pH 1, concentrated nitric acid was added to the freshly prepared alumina sol with pH  $\sim 6$ .

Silica sol at pH 2 was obtained from the passage of 500 mL of a 10% (m/v) aqueous sodium metasilicate solution (Nuclear) through a column full of cationic resin (IR 120, Rohm & Haas) in the  $H^+$  form.<sup>24</sup> The concentration of silicon in the resulting sol was determined by titration, as described in the literature.<sup>12</sup>

#### *Preparation of mullite precursors from mixtures of alumina and silica sols*

Amorphous mullite precursors were prepared by the sol-gel method, from mixtures of freshly prepared silica and alumina sols.

The compositions of the mullite precursors (Al:Si molar ratio) were 1:3 (excess of silica in comparison to stoichiometric mullite) and 3:1, corresponding to the stoichiometric mullite composition ( $3Al_2O_3 \cdot 2SiO_2$ ). The pH values of the mixtures were adjusted to 1, 4 and 8, with addition of concentrated nitric acid (PA, Merck) or ammonium hydroxide (PA, Mallinckrodt) and measured with indicator paper (Merck). These pH values were chosen based on the isoelectric points of the silica and alumina sols, respectively, of  $\sim 2$ <sup>12</sup> and  $\sim 7$ ,<sup>11</sup> and correspond to situations where silica and alumina sol particles were both positively (pH 1) or negatively (pH 8) charged and oppositely charged (pH 4), in order to evaluate the pH effect on mullite formation.

These mixtures of alumina and silica sols were submitted to heating at  $\sim 50$  °C in order to promote gel formation and drying. Their pH values were monitored and adjusted, when needed, until the materials dried. The dried materials were called mullite precursors.

#### *Mullite crystallization from amorphous precursors*

Subsequently, the amorphous mullite precursors were submitted to heating at 1050 °C for 50 h in a 3000/3P model (EDG) muffle oven. The heating started at room temperature, with a heating rate of 10 °C/min to reach  $1050 \pm 2$  °C. Some of the mullite precursors were previously heated at 450 °C for 4 h to eliminate the volatile organic material and others had their granulometry controlled ( $< 45 \mu m$ ). The resulting materials were characterized by the dynamic X-ray diffraction technique after thermal treatments at 1050, 1100, 1150 and 1200 °C.

#### *Characterization of materials*

The alumina sols at pH 1 and 6 were characterized by <sup>27</sup>Al Nuclear Magnetic Resonance (NMR) spectroscopy using approximately 2 mL of the sol in NMR tubes with diameter of 10 mm. <sup>27</sup>Al NMR experiments were performed at room temperature with a Bruker AC 300/P spectrometer, operating at 78.2 MHz, with delay of 0.5 s between pulses. The chemical shifts were relative to a 1.0 mol/L aqueous solution of aluminum nitrate defined at 0 ppm.

Photon Correlation Spectroscopy (PCS), using a ZetaPlus equipment (Brookhaven Instruments) and Bi-MAS software, determined both the effective particle diameters and the polydispersity of both the alumina and silica sols.

The powdered materials were characterized by powder X-ray diffraction, performed on a diffractometer (Shimadzu, model XRD 6000), using CuK $\alpha$  radiation, operating at 40 kV and 30 mA. Data were scanned between 5 and 70° ( $2\theta$ ) with a scanning rate of  $2\theta \text{ min}^{-1}$ . For X-ray dynamic studies at between 1050 and 1200 °C, the amorphous mullite precursors were submitted to a heating rate of 10 °C  $\text{min}^{-1}$  to 1050 °C. They were kept at this temperature for 5 min and the diffractogram of the materials were scanned. Then the materials were further heated at 2 °C  $\text{min}^{-1}$  to 1100 °C, kept for 5 min at this temperature before their diffractograms were scanned, heated at 2 °C  $\text{min}^{-1}$  to 1150 °C, and so on. Data were scanned from 10 to 50° ( $2\theta - \text{CuK}\alpha$ ), with a scanning rate of  $2\theta \text{ min}^{-1}$ .

## **Results and Discussion**

#### *Characterization of alumina and silica sols*

Figures 1 and 2 show the <sup>27</sup>Al Nuclear Magnetic Resonance spectra from the alumina sols, at pH  $\sim 6$  and 1, respectively.

In Figure 1, a broad peak located at 7.7 ppm and a sharp peak at 63.5 ppm, with a shoulder at 69.5 ppm are observed. The first peak corresponds to  $Al^{3+}$  ions with octahedral coordination while the others can be assigned to the  $Al^{3+}$  ions with tetrahedral coordination.<sup>28</sup> The sharp peak at 63.5 ppm, when compared to the broad peak at 7.7 ppm, indicates that the  $Al^{3+}$  ions are mainly tetrahedrally coordinated in the sol solution at pH 6.

In Figure 2, there is a sharp peak located at  $-5.8$  ppm and a broad peak at 63.5 ppm, which are assigned to the  $Al^{3+}$  ions, with octahedral and tetrahedral coordination, respectively. As the peak area integration of the octahedrally coordinated ions is greater than that of the tetrahedrally coordinated, there are mainly  $Al^{3+}$  ions

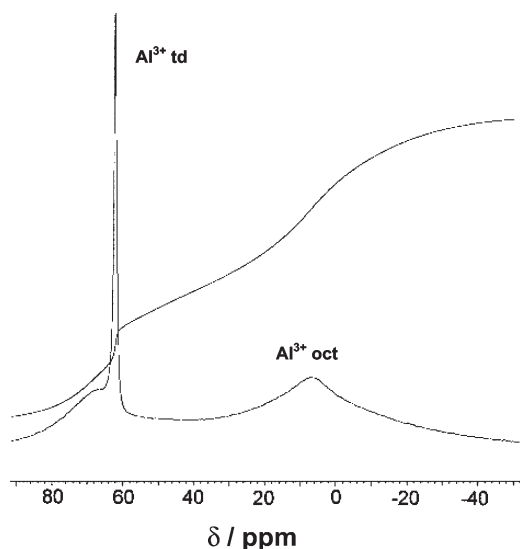


**Figure 1.**  $^{27}\text{Al}$  Nuclear Magnetic Resonance spectrum of the alumina sol at pH ~6.

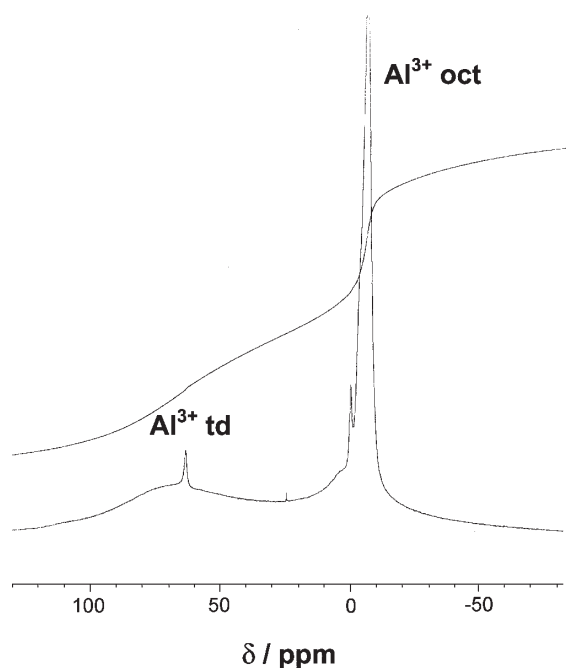


**Figure 2.**  $^{27}\text{Al}$  Nuclear Magnetic Resonance spectrum of the alumina sol at pH 1.

with octahedral coordination in the alumina sol solution at pH 1.

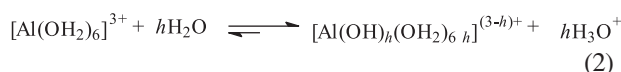
Table 1 presents the results of particle size and polydispersity of the silica and alumina sols, using the PCS technique.

From Table 1, it is observed that the particles present in the alumina sol (pH ~ 6) have bigger sizes than those of the alumina sol at pH 1. An increase in the pH value, due to the *in situ* generation of ammonia through urea thermolysis,<sup>21</sup> shown in equation 1, led to controlled

**Table 1.** Particle sizes and polydispersities of the silica and alumina sols

Sample	pH	Effective diameter (nm)	Sol polydispersity
Silica sol	2	47	0.434
Alumina sol	~ 6	196	0.092
Alumina sol	1	34	0.923

condensation of the  $\text{Al}^{3+}$  ion through ololation and oxolation mechanisms,<sup>14,28</sup> and resulted in polynuclear hydroxides or oxohydroxides, as indicated in equation 2, where  $h$  is defined as the molar ratio of hydrolysis.<sup>14</sup>



Previous studies have shown that a high concentration of urea in the initial steps of sol formation induced an intensive nucleation process, resulting in a narrow particle size distribution.<sup>26,29</sup> Thus, the alumina sol at pH ~6 showed a very narrow particle size distribution while the alumina sol at pH 1 present higher polydispersity. The distribution of particle sizes is related to the peptization of the larger alumina particles, giving rise to smaller ones or to  $\text{Al}^{3+}$  ions, as a result of  $\text{Al}^{3+}$  ion hydrolysis catalyzed by acid, indicated by the equilibrium shift of equation 2 to the left.<sup>14,27,28</sup> The  $\text{Al}^{3+}$  ion hydrolysis is controlled by the pH and results in the aluminum cation being coordinated to aquo ( $\text{H}_2\text{O}$ ) and/or hydroxo ( $\text{OH}^-$ ) ligands, as a function of the degree of hydrolysis.

From the NMR spectra and the particle size and the polydispersities of the alumina sols, a predominance of alumina particles containing  $\text{Al}^{3+}$  ions with mainly tetrahedral coordination was observed in the alumina sol at pH ~6. pH reduction causes the species in the alumina sol to change the  $\text{Al}^{3+}$  ion coordination from tetrahedral to octahedral, as well as inducing peptization of the alumina particles. This behavior can also be explained by  $\text{Al}^{3+}$  ion hydrolysis and condensation (equation 2).

#### Characterization of materials

Diffractograms of the materials obtained from amorphous mullite precursors with the Al:Si of 3:1 and 1:3 heated at  $1050 \pm 2$  °C for 50 h are shown, respectively, in Figures 3 and 4. Figure 5 shows the diffractograms of the materials heated at  $1050 \pm 2$  °C for 250 h.

The diffraction peak attributions, shown in Figures 3, 4 and 5, were performed by comparison of the peak

positions ( $2\theta$  -  $\text{CuK}\alpha$ ) with the ones given by JCPDS 27-0605, JCPDS 15-0776, JCPDS 46-1212 and JCPDS 47-1308, respectively, for cristobalite, mullite,  $\alpha$ -alumina and spinel and/or  $\gamma$ -alumina.

From the different diffractogram patterns shown in Figure 3 for the materials with the Al:Si molar ratio of 3:1 heated at  $1050 \pm 2^\circ\text{C}$  for 50 h, the pH must have influenced the phases formed. The diffractogram of the material obtained from the mullite precursor prepared at pH 1 presented some well resolved peaks, attributed to the  $\alpha$ -alumina phase, and one halo centered at  $\sim 22^\circ$  ( $2\theta$  -  $\text{CuK}\alpha$ ), characteristic of amorphous silica,<sup>8</sup> as well as broad peaks assigned to spinel and/or  $\gamma$ -alumina phases. On the other hand, only the spinel and/or  $\gamma$ -alumina segregation and amorphous silica were observed for the other materials, prepared at pH 4 and 8.

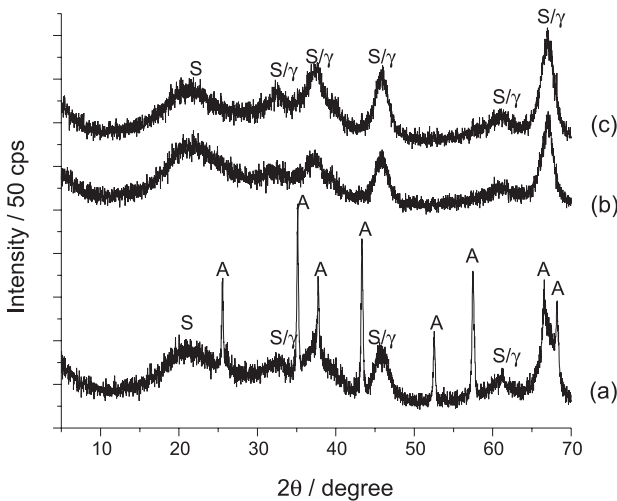


**Figure 3.** Diffractograms of the materials after heating mullite precursors, prepared with Al:Si = 3:1, at  $1050 \pm 2^\circ\text{C}$  for 50 h ((a) pH 1, (b) pH 4 and (c) pH 8 (A =  $\alpha$ -alumina, S/ $\gamma$  = spinel and/or  $\gamma$ -alumina, S = amorphous silica).

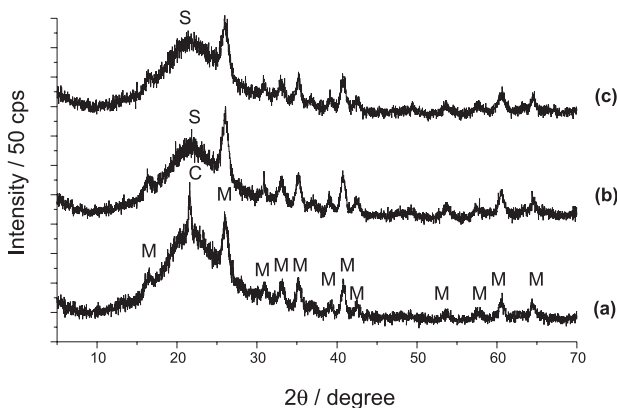


**Figure 4.** Diffractograms of the materials after heating mullite precursors, prepared with Al:Si = 1:3, at  $1050 \pm 2^\circ\text{C}$  for 50 h ((a) pH 1, (b) pH 4 and (c) pH 8 (C = cristobalite, M = mullite, S = amorphous silica).

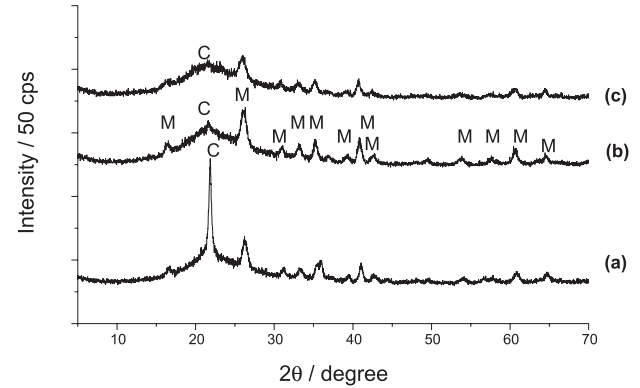


**Figure 5.** Diffractograms of the materials after heating mullite precursors, prepared with Al:Si = 1:3, at  $1050 \pm 2^\circ\text{C}$  for 250 h ((a) pH 1, (b) pH 4 and (c) pH 8 (C = cristobalite, M = mullite, S = amorphous silica).

In contrast to these materials, tetragonal mullite, characterized by only one peak at  $\sim 26^\circ$  ( $2\theta$  -  $\text{CuK}\alpha$ ), was formed from mixtures of silica and alumina sols with the Al:Si molar ratio of 1:3, as shown in the diffractograms of Figure 4. Segregation of amorphous silica and cristobalite phase, characterized, respectively, by an halo and a peak located at  $\sim 22^\circ$  ( $2\theta$  -  $\text{CuK}\alpha$ ) is also seen.

The diffractograms (Figure 5) of materials resulting from the mullite precursors with Al:Si = 1:3 heated at  $1050 \pm 2^\circ\text{C}$  for 250 h showed more defined cristobalite peaks, indicating a higher degree of crystallinity, especially for the precursor at pH 1, or a pattern at  $22^\circ$  more characteristic of a peak, instead of an halo, which can be attributed to cristobalite formation. The characteristic peaks of mullite did not seem to have significant increases in intensity, when compared to the diffractograms in Figure 4. The diffractograms shown in Figures 4 and 5 indicate that, for the mullite precursors with Al:Si = 1:3, the pH does not seem to play an important role on the phases formed.

Figures 6 to 8 show the diffractograms of the materials obtained from the mullite precursors with an Al:Si molar ratio of 3:1, prepared, respectively, at pH 1, 4 and 8, and submitted to the dynamic X-ray diffraction technique. The diffractograms indicate the formation of orthorhombic mullite, characterized by the splitting of the peak located at  $\sim 26^\circ$  ( $2\theta$  -  $\text{CuK}\alpha$ ), which refers to the 120 and 210 crystalline planes.<sup>30</sup>

Moreover, the diffractograms (Figures 6 to 8) show differences in the minimum temperatures for mullite crystallization for each mullite precursor under study. For the mullite precursor prepared at pH 8, the minimum temperature required for mullite formation was  $1100^\circ\text{C}$ , while for the others (prepared at pH 1 and 4), it was  $1150^\circ\text{C}$ .

The mullite precursor prepared at pH 8 had the lowest minimum temperature required for mullite formation. This

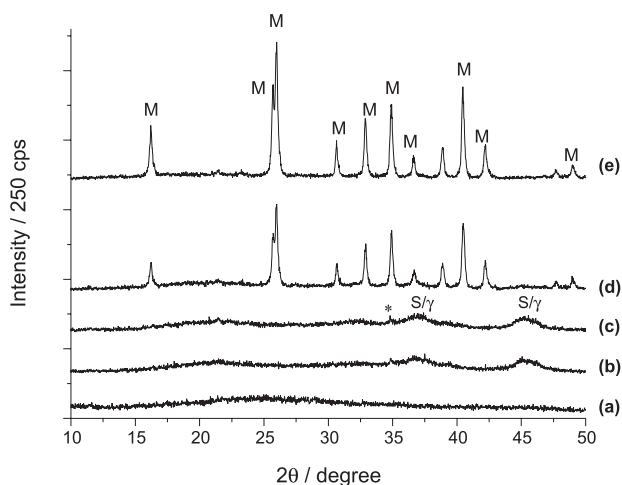


**Figure 6.** Dynamic X-Ray diffraction studies from a mullite precursor prepared at pH 1 ((a) 25 °C, (b) 1050 °C, (c) 1100 °C, (d) 1150 °C, (e) 1200 °C) (S/γ = spinel and/or γ-alumina, M = mullite, \*peaks from alumina sample holder).

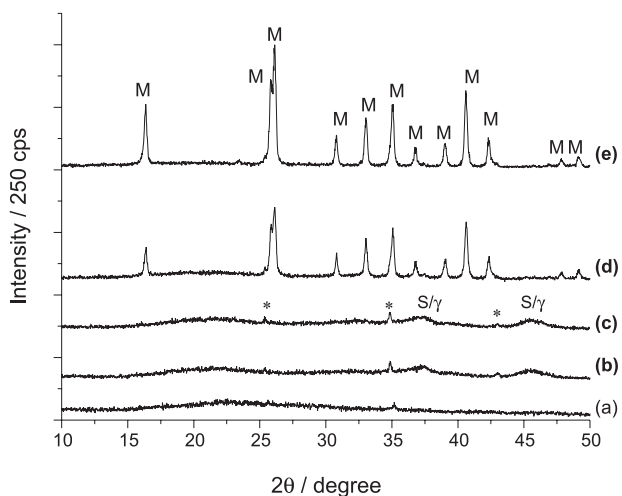


**Figure 7.** Dynamic X-Ray diffraction studies from a mullite precursor prepared at pH 4 ((a) 25 °C, (b) 1050 °C, (c) 1100 °C, (d) 1150 °C, (e) 1200 °C) (S/γ = spinel and/or γ-alumina, M = mullite, \*peaks from alumina sample holder).

result suggests that mullite formation from this precursor was more favorable than the others, requiring a smaller energy of activation, probably due its high degree of homogeneity. This result is reasonable in terms of homogeneity of this precursor, since there are negatively charged silica particles and a predominance of negatively charged alumina particles bigger than 196 nm diameter in the mixture of alumina and silica sols at pH 8. The electrostatic repulsion of silica and alumina particles, associated with the fact that the vast majority of the  $\text{Al}^{3+}$  ions are present in the sol particles, makes this precursor more homogeneous than the others.

In the mixture of alumina and silica sols at pH 1, which gave the mullite precursor at pH 1, there were mainly

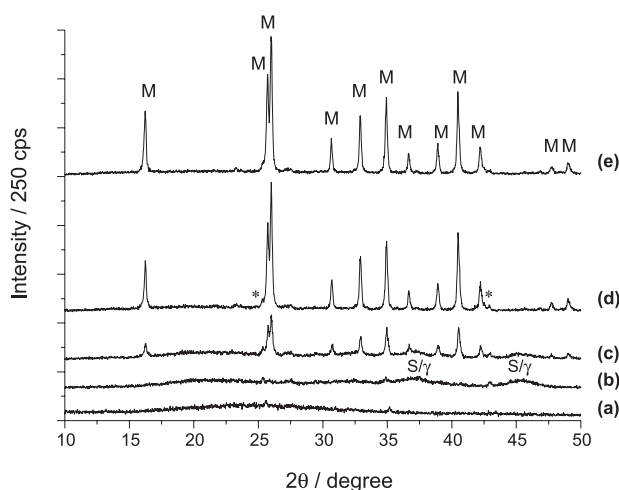


**Figure 8.** Dynamic X-Ray diffraction studies from a mullite precursor prepared at pH 8 ((a) 25 °C, (b) 1050 °C, (c) 1100 °C, (d) 1150 °C, (e) 1200 °C) (S/γ = spinel and/or γ-alumina, M = mullite, \*peaks from alumina sample holder).

tetrahedrally coordinated  $\text{Al}^{3+}$  ions with octahedral coordination present in solution, besides small alumina particles, according to the  $^{27}\text{Al}$  NMR and particle size data on the alumina sol. The majority of  $\text{Al}^{3+}$  ions did not interact with the alumina particles as particle-particle interactions, being dispersed in the medium. The positively charged alumina particles interacted with silica particles in this mixture and may have formed mullite under heating. Although the dynamic X-ray diffraction studies with this precursor showed only orthorhombic mullite formation, probably due to the different thermal treatments and conditions employed, it is reasonable to associate the higher temperature required for mullite formation with the low degree of homogeneity of this precursor, when compared to the precursor prepared at pH 8.

On the other hand, there are both alumina particles and positively charged  $\text{Al}^{3+}$  ions as well as negatively charged silica in the mixture prepared at pH 4. The large excess of aluminum species present, if compared to silica particles, led to a system consisting of a mixture of coagulated silica and alumina particles, as well as a dispersion of alumina particles or aluminum species. As this system had its alumina component less homogeneously distributed in the resulting precursor, it required higher activation energy and minimum temperature to crystallize to orthorhombic mullite than those for the precursor prepared at pH 8.

In addition to the pH effect on determining the minimum temperature required for mullite formation, the results in Figures 4 to 8 show that the mullite crystalline structures depend on the Al:Si molar ratio of the mullite precursors under study. Tetragonal mullite was crystallized from mullite precursors with Al:Si = 1:3, whereas

orthorhombic mullite was formed from the other mullite precursors, with Al:Si = 3:1. This difference in the structures of crystalline mullite may be related to the mechanism of mullite formation. In the mullite precursors with the Al:Si molar ratio of 1:3, there is an excess of silica, in comparison with the stoichiometric mullite composition (Al:Si = 3:1). Thus, it is reasonable to suggest that the mechanism for tetragonal mullite formation might be different from the mechanism that led to orthorhombic mullite formation.

Tetragonal mullite was crystallized from the mullite precursor with Al:Si = 1:3, prepared at pH 4 (Figures 4 and 5). At a pH the between alumina and silica isoelectric points (pH 4), the electrostatic attraction between alumina and silica particles may have enabled the alumina particles to be surrounded by the silica particles in excess in the mixture of the two sols, as shown in the schematic representation of Figure 9.<sup>22</sup>

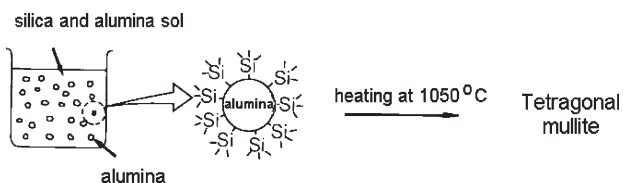


**Figure 9.** Schematic representation of tetragonal mullite formation from alumina and silica sol mixtures (Al:Si = 1:3).

In this case, coagulation took place slowly until all of the minority component (alumina) was used up. After gelling and drying, the system consisted of a mixture of two solid components (alumina and silica), surrounded by a dispersion of the component present in excess (silica). Consequently, tetragonal mullite must have formed from the total consumption of the alumina particles by the available silica, present in large excess. The unreacted silica then led to cristobalite or amorphous silica formation.

However, tetragonal mullite formation was also verified from mullite precursors prepared at pH 1 and 8, where both alumina and silica particles present positive or negative charges, respectively. These results suggest that mullite formation was not governed by the interaction of these particles. The large excess of silica must have affected their distribution, overcoming the interaction between particles, determined by the pH.

According to Iler,<sup>31</sup> when one kind of particle is present in large excess, the particles in minority become covered with the particles that are in excess. From this assumption, the distribution of alumina and silica particles in the precursors prepared at pH 1 and 8 were similar to the scheme shown in Figure 9. As a consequence, it is reasonable to suppose that the nature of the interactions between these

particles would not exert great influence on the phases formed and/or on the temperature required for mullite formation. These assumptions were confirmed since the diffractograms of all materials with Al:Si = 1:3 were very similar (Figures 4 and 5) and it can be inferred that the pH did not influence the degree of homogeneity of these mullite precursors. In addition, from the schematic representation (Figure 9), tetragonal mullite formation has the alumina dissolution as the limiting step of mullite formation from diphasic gels, as proposed by Sundaresan and Aksay.<sup>18</sup>

On the other hand, the mechanism for orthorhombic mullite formation from the precursors with the Al:Si molar ratio of 3:1 (stoichiometric composition of mullite) must be related to alumina and silica particle interactions, as a consequence of the role of the pH on determining the charges of the alumina and silica particles, as well as on the predominant aluminum species.

## Conclusions

Tetragonal mullite formation from mullite precursors with the Al:Si molar ratio of 1:3, prepared by the sol-gel method from mixtures of alumina and silica sols at different pH values, was well represented by the mechanism proposed by Sundaresan and Aksay, with alumina dissolution on silica as the determining step for mullite formation. In this case, the pH effect in determining the charges on alumina and silica particles and, thus, their interactions was minimized. The excessive concentration of silica determined the distributions of the components present in the Al:Si = 1:3 mullite precursors.

On the other hand, the pH played an important role on the precursors with the Al:Si molar ratio of 3:1. The pH determined not only the interactions of silica and alumina particles, but also the predominant aluminum species, either Al<sup>3+</sup> ions with octahedral coordination or tetrahedrally coordinated Al<sup>3+</sup> ions. The resulting degree of homogeneity of these mullite precursors affected the minimum temperature required for orthorhombic mullite formation.

## Acknowledgements

The authors thank Capes for financial support.

## References

- Gerardin, C.; Sundaresan, S.; Benziger, J.; Navrotsky, A.; *Chem. Mater.* **1994**, *6*, 160.
- Aksay, I. A.; Dabbs, D. M.; Sarikaya, M.; *J. Am. Ceram. Soc.* **1991**, *74*, 2343.

3. Schneider, H.; Saruhan, B.; Voll, D.; Merwin, L.; Sebald, A.; *J. Eur. Ceram. Soc.* **1993**, *11*, 87.
4. Kim, J. W.; Lee, J. E.; Jung, Y. G.; Jo, C. Y.; Lee, J. H.; Paik, U.; *Mater. Res. Soc.* **2003**, *18*, 81.
5. Satoshi, S.; Contreras, C.; Juárez, H.; Aguilera, A.; Serrato, J.; *Int. J. Inorg. Mater.* **2001**, *3*, 625.
6. Mazel, F.; Gonon, M.; Fantozzi, G.; *J. Eur. Ceram. Soc.* **2002**, *22*, 453.
7. Vol'khin, V. V.; Kazakova, I. L.; Halwax, E.; Pongratz, P.; *Russ. J. Gen. Chem.* **1999**, *69*, 1861.
8. Padmaja, P. Anilkumar, G. M.; Mukundan, P.; Aruldas, G.; Warriar, K.G.K.; *Int. J. Inorg. Mater.* **2001**, *3*, 693.
9. Li, D. X.; Thomson, W. J.; *J. Am. Ceram. Soc.* **1991**, *74*, 2382.
10. Skoog, A. J.; Moore, R. E.; *Am. Ceram. Soc. Bull.* **1988**, *67*, 1180.
11. Wang, G. H.; Nicholson, P. S.; *J. Am. Ceram. Soc.* **2001**, *84*, 1250.
12. Iler, R. K.; *The Chemistry of Silica*; John Wiley & Sons, Inc.: New York, 1979.
13. Islam, A. M.; Chowdhry, B. Z.; Snowden, M. J.; *Adv. Colloid Interface Sci.* **1995**, *62*, 109.
14. Brinker, C. J.; Scherer, G. W.; *Sol-Gel Science – the Physics and Chemistry of Sol-Gel Processing*; Academic Press, Inc.: Boston, 1990.
15. Lee, J. E.; Kim, J. K.; Jung, Y. G.; Jo, C. Y.; Paik, U.; *Ceram. Int.* **2003**, *28*, 935.
16. Rahaman, M. N.; De Jonghe, L. C.; Shinde, S. L.; Tewari, P. H.; *J. Am. Ceram. Soc.* **1988**, *71*, C-338.
17. Chu, L.; Tejedor-Tejedor, M. I.; Anderson, M. A.; *Microporous Mater.* **1997**, *8*, 207.
18. Sundaresan, S.; Aksay, I. A.; *J. Am. Ceram. Soc.* **1991**, *74*, 2388.
19. Vollet, D. R.; Donatti, D. A.; Domingos, R.N.; de Oliveira, I.; *Ultrason. Sonochem.* **1998**, *5*, 79.
20. Jaymes, I.; Douy, A.; Massiot, D.; *J. Am. Ceram. Soc.* **1995**, *78*, 2648.
21. Wang, K.; Sacks, M. D.; *J. Am. Ceram. Soc.* **1996**, *79*, 12.
22. Okada, S.; Otsuka, N.; Somiya, S.; *Am. Ceram. Soc. Bull.* **1991**, *70*, 1633.
23. Hong, S. H.; Messing, G. L.; *J. Am. Ceram. Soc.* **1998**, *81*, 1269.
24. Osawa, C. C.; *M.Sc. Dissertation*, Universidade Estadual de Campinas, Brazil, 2004.
25. Li, D. X.; Thomson, W. J.; *J. Mater. Res.* **1991**, *6*, 819.
26. Macêdo, M. I. F.; Osawa, C. C.; Bertran, C. A.; *J. Sol-Gel Sci. Technol.*, **2004**, *30*, 135.
27. Akitt, J. W.; Mann, B. E.; *J. Magn. Res.* **1981**, *44*, 584.
28. Jansen, J.C. In *Advanced Zeolite Science and Applications*; Stocker, H. G.; Karge, J. W., eds., Elsevier Science B.V.: Amsterdam, 1994.
29. Thim, G. P.; Bertran, C. A.; Barlette, V. E.; Macêdo, M. I. F.; Oliveira, M. A. S.; *J. Eur. Ceram. Soc.* **2001**, *21*, 759.
30. Johnson, B. R.; Kriven, W. M.; Shneider, J.; *J. Eur. Ceram. Soc.* **2001**, *21*, 2541.
31. Iler, R. K.; *J. Am. Ceram. Soc.* **1964**, *47*, 194.

Received: May 21, 2004

Published on the web: February 21, 2005

FAPESP helped in meeting the publication costs of this article.